Available online at www.sciencedirect.com
SCIENCE DIRECT®
Colloids and Surfaces B: Biointerfaces 42 (2005) 157–174
COLLOIDS AND SURFACES B
www.elsevier.com/locate/colsurfb

Cerebroside Langmuir monolayers originated from the echinoderms I. Binary systems of cerebrosides and phospholipids

Hiromichi Nakahara [a], Shohei Nakamura [a], Kazufumi Nakamura [b], Masanori Inagaki [b], Mariko Aso [c], Ryuichi Higuchi [b], Osamu Shibata [a,*]

[a] *Division of Biointerfacial Science, Graduate School of Pharmaceutical Sciences, Kyushu University, 3-1-1 Maidashi, Higashi-ku, Fukuoka 812-8582, Japan*
[b] *Natural Products Chemistry, Graduate School of Pharmaceutical Sciences, Kyushu University, 3-1-1 Maidashi, Higashi-ku, Fukuoka 812-8582, Japan*
[c] *Pharmaceutical Synthetic Chemistry, Graduate School of Pharmaceutical Sciences, Kyushu University, 3-1-1 Maidashi, Higashi-ku, Fukuoka 812-8582, Japan*

Received 10 November 2004; accepted 29 January 2005
Available online 16 March 2005

Abstract

The surface pressure (π)–area (A), the surface potential (ΔV)–A and the dipole moment ($\mu_\perp$)–A isotherms were obtained for two-component monolayers of two different cerebrosides (LMC-1 and LMC-2) with phospholipids of dipalmitoylphosphatidylcholine (DPPC) and with dipalmitoylphosphatidylethanolamine (DPPE) on a subphase of 0.5 M sodium chloride solution as a function of phospholipid compositions by employing the Langmuir method, the ionizing electrode method, and the fluorescence microscopy. Surface potentials (ΔV) of pure components were analyzed using the three-layer model proposed by Demchak and Fort [J. Colloid Interf. Sci. 46 (1974) 191–202]. The contributions of the hydrophilic saccharide group and the head group to the vertical component of the dipole moment ($\mu_\perp$) were estimated. The miscibility of cerebroside and phospholipid in the two-component monolayers was examined by plotting the variation of the molecular area and the surface potential as a function of the phospholipid molar fraction ($X_{\text{phospholipid}}$), using the additivity rule. From the A–$X_{\text{phospholipid}}$ and ΔV_{m}–$X_{\text{phospholipid}}$ plots, partial molecular surface area (PMA) and apparent partial molecular surface potential (APSP) were determined at the discrete surface pressure. The PMA and APSP with the mole fraction were extensively discussed for the miscible system. Judging from the two-dimensional phase diagrams, these can be classified into two types. The first is a positive azeotropic type; the combinations of cerebrosides with DPPC are miscible with each other. The second is a completely immiscible type: the combination of cerebrosides with DPPE. Furthermore, a regular surface mixture, for which the Joos equation was used for the analysis of the collapse pressure of two-component monolayers, allowed calculation of the interaction parameter (ξ) and the interaction energy ($-\Delta\varepsilon$) between the cerebrosides and DPPC component. The miscibility of cerebroside and phospholipid components in the monolayer state was also supported by fluorescence microscopy.

Keywords: Langmuir monolayer; Glycosphingolipids; Cerebrosides; Phospholipids; Surface dipole moment ($\mu_\perp$); π–A isotherm; ΔV–A isotherm; Two-dimensional phase diagram; Fluorescence microscopy

1. Introduction

The functions of animal cells at their surfaces regulate such fundamental biological processes as growth, differentiation, and motility. Although the nature of the functions is not understood at the molecular level, it is understood that the complex glycolipid and glycoprotein molecules sitting at the outer surface of the cells are involved. Lipid molecules containing sugar groups are called glycosphingolipids. Glycosphingolipids (GSLs) are present in most animal cell plasma membranes and are thought to play a role in a number of cellular functions, including cell recognition, adhesion, regulation, signal transduction, and development of tissues. They predominantly locate on the outer leaflet of the membrane and may act to protect the membrane from harsh conditions such

DOI of original article:10.1016/j.colsurfb.2005.01.013.
* Corresponding author. Tel.: +81 92 642 6669; fax: +81 92 642 6669.
E-mail address: shibata@phar.kyushu-u.ac.jp (O. Shibata).
URL: http://kaimen.phar.kyushu-u.ac.jp/.

0927-7765/$ – see front matter © 2005 Elsevier B.V. All rights reserved.
doi:10.1016/j.colsurfb.2005.01.012

as a low pH or degradative enzymes [1]. A detailed description of the chemical, structural, and functional properties of glycolipids in general can be found in a review article by Mggio [2].

Glycosphingolipids (cerebrosides) are amphiphilic compounds consisting of saccharide and ceramide moieties and are ubiquitous components of the plasma membrane of all eucaryotic cells [3,4]. Glycosphingolipids are considered to be receptors for microorganisms and their toxins, modulators of cell growth, and differentiation, and organizers of cellular attachment to matrices [5,6]. Recent cell biological studies show that cerebrosides in plasma membranes form clusters, the so-called rafts, with cholesterol and are relatively less phospholipids than other areas of plasma membrane. Glycosphingolipids could mediate the signal transduction pathway through interaction with these signaling proteins and not only circulate between the plasma membrane and intracellular organs but also move laterally over the exoplasmic membrane. Such migration could be conducted by raft [7,8]. Glycosphingolipids [9–13] are a major component of the myelin sheath [14–16]. Glucocerebrosides and lactosylceramide are the major extraneural glycosphingolipids [17–19]. GSLs with tri- and tetrasaccharide-containing head groups, known as globosides, are found in the erythrocyte membrane [20]. GSLs show heterogeneity not only in their saccharide head group, but also in their ceramide moieties. The biological significance of ceramide heterogeneity is not still understood well. However, especially the structure of ceramide for the fatty acid moieties could influence the localization and functions of GSLs on the plasma membrane, possibly by direct interaction with cholesterol, phospholipids, and the transmembrane domains of receptor proteins [21–24]. Unusual structures of GSLs will be revealed in future through further technological innovation.

However, the organization of cerebroside–phospholipid mixtures is quite unclear. As long as we know, reports on cerebrosides are still much fewer in number than reports on gangliosides [25]. In the previous studies, we have only restricted a two-component monolayer system of sphingolipid (cereboroside:LMC-2), cholesteryl sodium sulfate (Ch-S), and cholesterol and their combinations as to monolayer properties of surface pressure– and surface potential–surface area at the air/water interface without fluorescence microscopy measurements [26].

Here, we have focused on characterizing the Langmuir behavior of some pure cerebrosides, phospholipids, and their two-component systems at air/water interface. Surface pressure (π)–, surface potential (ΔV)–, and dipole moment ($\mu_{\perp}$)–A isotherms were obtained for the pure compounds and their two-component systems. The surface potentials were analyzed using the three-layer model proposed by Demchak and Fort [27]. The phase behavior of two-component monolayers was examined in terms of additivity of molecular surface area and of surface potential. Furthermore, it was analyzed employing the partial molar molecular area (PMA) and apparent partial molar surface potential (APSP). The molecular interaction between monolayer components was investigated using the Joos equation. Finally, the monolayers were examined by fluorescence microscopy. Similar analyses are reported for binary cerebroside – steroid monolayers in the following articles in series.

2. Experimental

2.1. Materials

The cerebrosides (PA-0-5, LMC-1, and LMC-2) possess β-*O*-glucosyl head group linked to the terminal hydroxyl group of ceramide. These compounds were obtained from the less polar fraction of the extract of the echinoderms. PA-0-5 was extracted from the sea cucumber *Pentacta australis* (Gokakukinko in Japanese). The chemical structure of this compound has been already identified [28]. On the other hand, LMC-1 and LMC-2 were obtained from the starfish *Luidia maculata* (Yatsudesunahitode in Japanese). These compounds (LMC-1 and LMC-2) were molecular species [19]. LMC-1 has double bonds in the hydrophobic chains. By hydrogenation with Pd/C in *n*-hexane/EtOH (1:1, v/v), LMC-1 was converted into sphinganine (LMC-1-H) that has two saturated hydrophobic chains. All cerebrosides were checked by ^{1}H- and ^{13}C-NMR spectra after purification by TLC and HPLC. The compositions of the hydrophobic acyl chain and long chain base (LCB) are given in Table 1. In Fig. 1, *n* and *m* are the number of carbon atoms of the acyl chain and long chain base, respectively. Dipalmitoylphosphatidylcholine(L-α-1-palmitoyl-2-hydroxy-*sn*-glycero-3-phosphocholine, DPPC) was purchased from Avanti Polar Lipids, Inc. (Birmingham, Alabama, U.S.A.) and dipalmitoylphosphatidylethanolamine(L-α-1-palmitoyl-2-hydroxy-*sn*-glycero-3-phosphoethanolamine, DPPE) was obtained from NOF Corporation (Japan). Their purity was >99%. All phospholipids were checked by TLC just before their use and used without further purification. The chemical structures of the cerebrosides used are shown in Fig. 1.

Table 1
Acyl chain and long chain base (LCB) compositions of cerebrosides

	Composition (%)		
	PA-0-5	LMC-1	LMC-2
Acyl chain			
22	100 (22:0)	56.8	56.0
23		34.7	35.5
24		8.5	8.5
LCB part			
16 (m = 11)		9.6	
17 (m = 12)	100 (17:1)	38.5	5.3
18 (m = 13)		16.0	12.2
19 (m = 14)		35.9	82.5

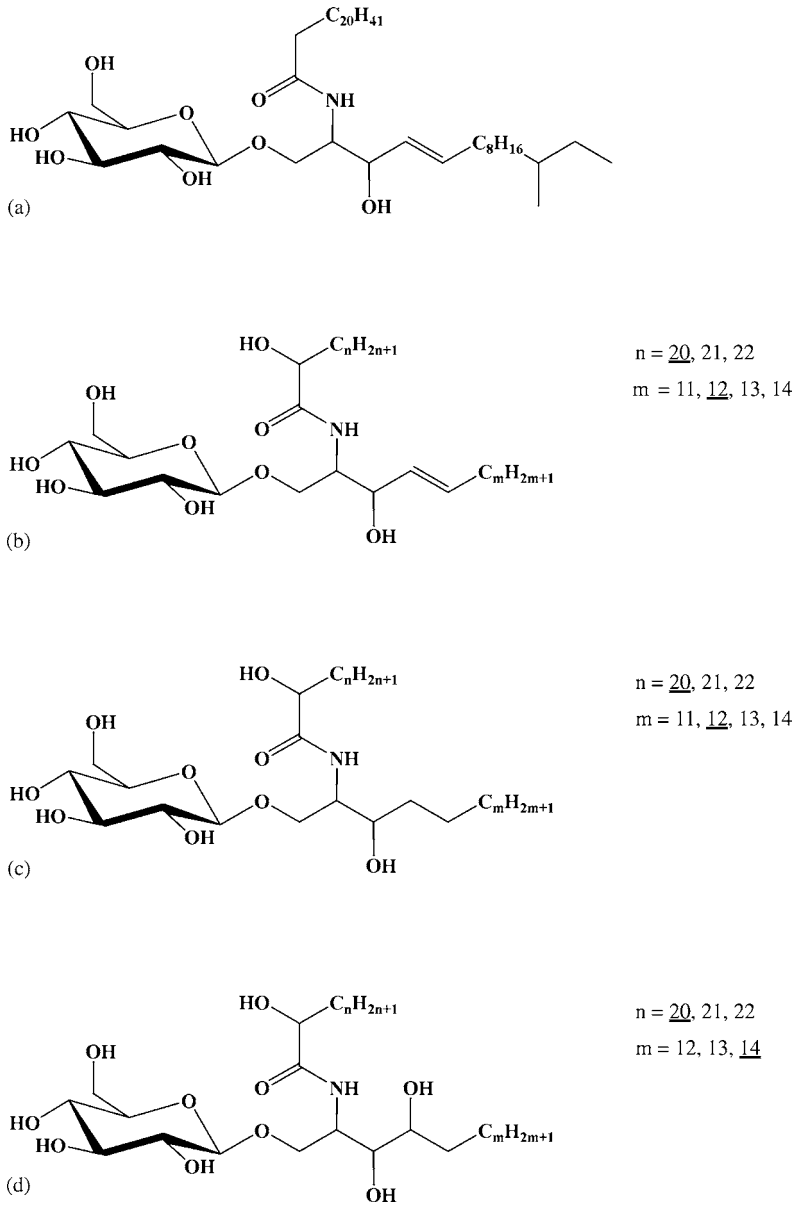

Fig. 1. Chemical structures of the cerebroside molecules studied: (a) PA-0-5; (b) LMC-1; (c) LMC-1-H; (d) LMC-2. *n* and *m* show the carbon number and underbars indicate the major component of the molecular species.

After the samples were dried in a vacuum desiccator containing phosphorus pentaoxide (Nacalai tesque), stock solutions of these samples were prepared in about 0.065 mM by using a microbalance (Mettler Toledo, AT21 Comparator) and gas-tight syringe (Dynatech). Specimens were dissolved in *n*-hexane/ethanol mixture (7/3, v/v; the former from Cica-Merck, Uvasol, and the latter from Nacalai Tesque).

The subphase of 0.5 M sodium chloride, presumed seawater, was prepared using triple distilled water. The first distillation was practiced with an addition of potassium permanganate (Nacalai tesque) for the purpose to remove organic substances in tab water. Sodium chloride was roasted at 1023 K for 24 h to remove any surface-active organic impurity.

2.2. π–*A and* ΔV–*A measurements*

The surface pressure (π) was measured by automated Langmuir film balance. A resolution of its balance (Cahn RG, Langmuir float type) is 0.01 mN m^{-1}. The trough was made from aluminum coated with Teflon and its dimension was 500 mm × 150 mm. Before each experiment, the trough was rinsed and cleaned with acetone and chloroform, respectively. The absence of surface-active compounds in the subphase (0.5 M NaCl, about pH 6.5) was checked by reducing the available surface area to less than 4% of its original area after sufficient time was allowed for adsorption of possible impurities that might be present by trace amounts in the substrate. Only substrate that did not show changes of surface

pressure above 0.5 mN m^{-1} and of surface potential 50 mV on this procedure was used. A monolayer was prepared by spreading a 100-μL solution at 298.2 K. A period of time, 15 min was needed to evaporate the spreading solvent, and then the monolayer was compressed at a constant rate of 1.00×10^{-1} nm^2 molecule^{-1} min^{-1}.

Surface potential (ΔV) was simultaneously recorded while the monolayer was compressed. It was measured with an electrometer (Keithley, 614) and ^{241}Am air-ionizing electrode at 1–2 mm above the interface, while a reference electrode was dipped in subphase. Reproducibility was within ±0.05 nm^2, ±0.1 mN m^{-1}, and ±5 mV for molecular area, surface pressure, and surface potential, respectively. Other experimental conditions were the same as described in the previous paper [29].

2.3. Fluorescence microscopy

Fluorescence images were observed using the automated Langmuir film balance equipped with a fluorescence microscope (BM-1000, U.S.I. System, Japan). It is possible to record simultaneously the surface pressure (π)–area (A) and the surface potential (ΔV)–A isotherms along with the monolayer images to correlate these properties of the same monolayer. A 300-W lamp (XL 300, pneum) was used for fluorescence excitation. A 546-nm band pass filter (Mitutoyo) was used for excitation and a 590 nm cut-off filter (Olympus) for emission. The monolayer was observed using a 20× long-distance objective lens (Mitutoyo f = 200/focal length 20 mm). A xanthylium 3,6-bis(diethylamino)-9-(2-octadecyloxycarbonyl)phenyl chloride (R18, Molecular Probes) was used as an insoluble fluorescent probe. It has its absorbance and emission band maxima at 556 and 578 nm, respectively. The solution used in the fluorescence microscopy experiments contained 1 mol% of the fluorescent probe against insoluble materials. Fluorescence images were recorded with a CCD camera (757 JAI ICCD camera, Denmark) connected to the microscope, directly into computer memory through an online image processor (VAIO PCV-R53, Sony: video capture soft). All the experiments were carried out in a dark room at 298.2 K. Image analysis was performed using NIH image (developed at the U.S. National Institutes Health). All images presented appear without image enhancement.

3. Results and discussion

3.1. π–A and ΔV–A isotherms of cerebroside and phospholipid monolayers

The π–A, ΔV–A, and $\mu_\perp$–A isotherms of monolayers made from pure cerebrosides (PA-0-5, LMC-1, LMC-1-H, and LMC-2) and phospholipids (DPPC and DPPE) spread on 0.5 M NaCl solution at 298.2 K are shown in Fig. 2. Surface areas of the cerebrosides (glycosphingolipids) were larger than those of phospholipids. The high compressibility of the cerebrosides over the whole surface pressures and the absence of discontinuities in their π–A isotherms show that they are typical liquid-expanded (LE) monolayer (Fig. 2A). All cerebrosides employed in this study possess an identical hydrophilic head group. Differences of average molecular areas result from variation in the packing state of the hydrophobic chains slight olefin and branching chain parts. The long-chain base of PA-0-5 consists of a 14-methylhexadecane derivative, while the long-chain base of LMC-1 and LMC-2 is mixtures of various chain lengths. So, the π–A isotherms of PA-0-5 occupied larger area than any other cerebrosides and was stable up to 41 mN m^{-1}. The extrapolated area in the closed pack state was 0.68 nm^2, and the collapse area was 0.48 nm^2. LMC-1 and LMC-2 contain an unsaturated hydrocarbon chain and their double bonds were *trans*-type. The extrapolated area and the collapse area of their π–A isotherms were 0.65 and 0.56 nm^2 for LMC-1 and 0.41 and 0.38 nm^2 for LMC-2. LMC-1-H has no double bond owing to hydrogenation of LMC-1, and the extrapolated area and the collapse area were 0.50 and 0.32 nm^2, respectively. The collapse pressures of these cerebrosides were almost same, about 50 mN m^{-1}.

On the other hand, the DPPC isotherm presented the characteristic first-order transition from the disordered LE phase to the ordered liquid-condensed (LC) phase (Fig. 2B). The transition pressure, π^{eq} at 298.2 K was 10.5 mN m^{-1}, above which the surface pressure rose due to the orientational change. Collapse of the DPPC monolayer occurred at 59 mN m^{-1}, and the extrapolated area was 0.52 nm^2. DPPE exhibited a liquid-condensed (LC) monolayer, its collapse pressure was 53 mN m^{-1} and the extrapolated area was 0.46 nm^2.

The surface potential (ΔV) is a measure of the electrostatic field gradient perpendicular to the surface and thus varies considerably with the molecular surface density. The behaviors of ΔV–A isotherms for cerebrosides correspond to the change of the molecular orientation upon compression as shown in Fig. 2A. The surface potentials (ΔV) of cerebrosides showed always positive. The PA-0-5 monolayer showed the largest variation of ΔV under compression among them, which reached a value of around 320 mV at the closest packed state. The LMC-2 monolayer showed the smallest ΔV value of 110 mV at high surface pressure.

The vertical component of surface dipole moment, $\mu_\perp$, was calculated from the Helmholtz equation using the measured ΔV values:

$$\Delta V = \mu_\perp / \varepsilon_0 \varepsilon A \quad (1)$$

where ε_0 is the permittivity of a vacuum and ε the mean permittivity of the monolayer (which is assumed to be 1). A is the area occupied by the molecule. The ΔV values involve the resultant of the dipole moments carried by the polar head (saccharide), the C–H bond (the CH_3 group), and the subphase. As the subphase and the hydrophilic head

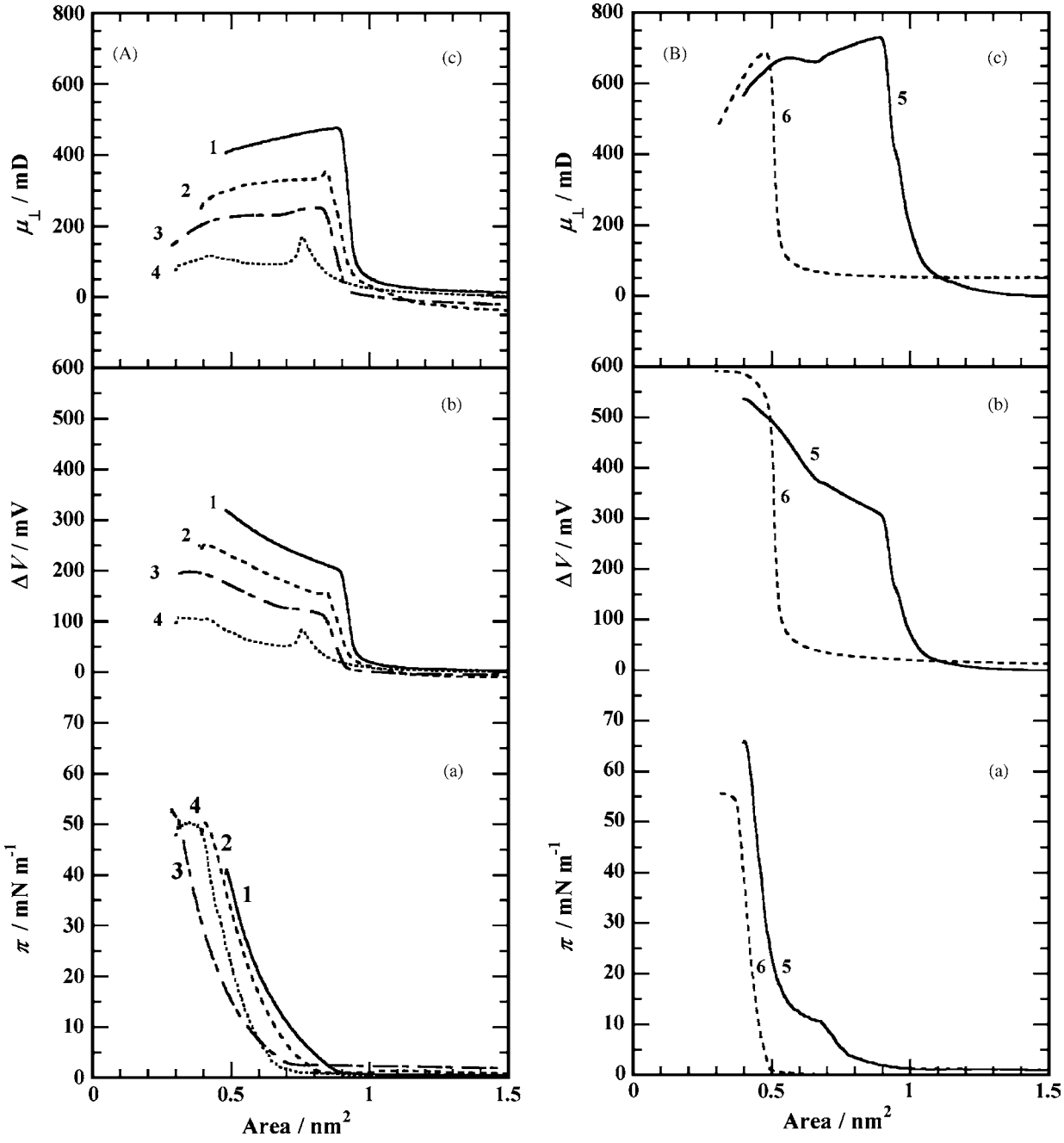

Fig. 2. Surface pressure (π)–area (A) isotherms (a), surface potential (ΔV)–A isotherms (b), and surface dipole moment ($\mu_\perp$)–A isotherms (c) of cerebrosides (A) and phospholipids (B) on 0.5 M NaCl at 298.2 K; (1) PA-0-5, (2) LMC-1, (3) LMC-1-H, (4) LMC-2, (5) DPPC, and (6) DPPE.

are identical for the present four cerebrosides, the difference observed in the ΔV values for the cerebrosides clearly evidences the magnitude of influence of the hydrophobic tails.

3.2. The surface dipole moments ($\mu_\perp$) of cerebrosides

The surface potential of monolayers was often analyzed using the three-layer model proposed by Demchak and Fort [27], which is based on the earlier model of Davies and Rideal [30]. This model postulates independent contributions of the subphase (layer 1), polar head group (layer 2), and hydrophobic chain (layer 3). Independent dipole moments and effective local dielectric constants are attributed to each of the three layers. Other models, such as the Helmholtz model and the Vogel and Möbius model are also available [31]. These different models were reviewed in Ref. [29]. The conclusion was that, despite its limitations, the Demchak and Fort model provided good agreement between the $\mu_\perp$ values estimated from the monolayer surface potentials and those determined from measurements on bulk material for various aliphatic compounds.

The estimation of $\mu_\perp$ (the vertical components of the dipole moment to the plane of the monolayer) of polar head groups and hydrocarbon chains using the Demchak and Fort model assumes a condensed Langmuir monolayer of close-packed vertical chains [27,30]. Application of this model to the cerebrosides LE monolayer may lead to a rough estimation. However, if the value of closest-packed cerebrosides monolayer is applied to this model, it may lead to a useful estimation, which can help to provide qualitative explanation of surface potential behavior.

We have thus compared the experimental values of $\mu_\perp$ in the most condensed state of the monolayer with those calculated $\mu_{\perp\text{calc}}$ by the three-layer model-based equation:

$$\mu_{\perp_{\text{calc}}} = \mu_1/\varepsilon_1 + \mu_2/\varepsilon_2 + \mu_3/\varepsilon_3 \quad (2)$$

where μ_1/ε_1, μ_2/ε_2, and μ_3/ε_3 are the contributions of the subphase, polar head group, and hydrophobic chain group, respectively.

We want to determine the contribution of the hydrophobic group of cerebroside and saccharide of hydrophilic group separately. Carboxylic and hydroxyl groups have already been determined by the Demchak and Fort model [27].

The initial set of values proposed by Demchak and Fort ($\mu_1/\varepsilon_1 = 0.040$ D, $\varepsilon_2 = 7.6$, and $\varepsilon_3 = 5.3$ [27]) was determined for monolayers made from terphenyl derivatives and octadecyl nitrile. Another set of values was determined in the papers by Petrov et al. ($\mu_1/\varepsilon_1 = 0.025$ D, $\varepsilon_2 = 7.6$, and $\varepsilon_3 = 4.2$ [32]) for monolayers of *n*-heptanol and 16-bromohexadecanol. We have used a set of values introduced by Taylor et al. ($\mu_1/\varepsilon_1 = -0.065$ D, $\varepsilon_2 = 6.4$, and $\varepsilon_3 = 2.8$) for monolayers of ω-halogenated fatty acids and amines [33].

To determine the set of the parameters of our experimental condition, the selection of parameter values was done using the standard sample of stearic acid (SA). In the first approximation, we assume that they are constant independent of the nature of the head group so that they may be evaluated from the data on stearic acid. These data are listed in Table 2. The experimental values of surface dipole moment for stearic acid (SA) used to determine the set of the parameters were as follows:

$$\mu_\perp(\text{SA}) = \mu_1/\varepsilon_1 + \mu_2^{\text{COOH}}/\varepsilon_2 + \mu_3^{\text{CH}_3}/\varepsilon_3 = 0.16\,\text{D} \quad (3)$$

In the calculation, it was assumed that the C–X dipole of terminal $-CH_2X$ moiety (where X is a hydrogen) was inclined at half the tetrahedral angle (i.e. 54°44′) with respect to the water surface as suggested by Bernett et al. [34] and that the group moments have the values given by Smyth [35]. In addition, it was assumed that the C–H group moment was 0.4 D, the carbon being negatively charged [36]. So the contribution of terminal methyl group is 0.33 D. The values have been proposed for μ_2 for the different conformations of the COOH group: μ_2(COOH–α *cis*(*cis*) acid) = 0.82 D, μ_2(COOH–α *trans*(*cis*) acid) = −0.64 D, μ_2(COOH–α *cis*(*trans*) acid) = 3.56 D, μ_2(COOH–α *trans*(*trans*) acid) = 0.99 D, μ_2(COOH–α *cis*(free) acid) = 2.36 D, and μ_2(COOH–α *trans*(free) acid) = 0.25 D [28]. Here, we have used μ_2(COOH–α *cis*(*cis*) acid) = 0.82 D value, because they provide a good agreement between calculated values and experimental values of dipole moments measured on a saline phase. The authors have used the combination of the set of values ($\mu_1/\varepsilon_1 = -0.065$ D, $\varepsilon_2 = 6.4$, and $\varepsilon_3 = 2.8$).

Second, we evaluated the contribution of the hydrophobic tail and the hydrophilic head group of cerebrosides.

$$\mu_\perp(\text{PA-0-5}) = \mu_1/\varepsilon_1 + \mu_2^{\text{sac}}/\varepsilon_2 + \mu_3^{\text{PA-0-5}}/\varepsilon_3 = 0.41\,\text{D} \quad (4)$$

We thought here that the structure of PA-0-5 was already identified and not molecular species, then the contribution of hydrophobic group of PA-0-5 depends on both the two terminal methyl groups and one vertical of C–H bond. So we can get 1.06 D for μ_2^{sac}. Inserting this value to Eq. (4), the contribution of the saccharide part was 0.63 D. Next the hydrophilic groups of three cerebrosides (LMC-1, LMC-1-H, and LMC-2) are the same as the group of PA-0-5, and therefore, we can evaluate the value of hydrophobic parts ($\mu_3^{\text{LMC-1}}$, $\mu_3^{\text{LMC-1-H}}$, and $\mu_3^{\text{LMC-2}}$) using Eqs. (5)–(7), respectively:

$$\mu_\perp(\text{LMC-1}) = \mu_1/\varepsilon_1 + \mu_2^{\text{sac}}/\varepsilon_2 + \mu_3^{\text{LMC-1}}/\varepsilon_3 = 0.28\,\text{D} \quad (5)$$

$$\mu_\perp(\text{LMC-1-H}) = \mu_1/\varepsilon_1 + \mu_2^{\text{sac}}/\varepsilon_2 + \mu_3^{\text{LMC-1-H}}/\varepsilon_3 = 0.17\,\text{D} \quad (6)$$

$$\mu_\perp(\text{LMC-2}) = \mu_1/\varepsilon_1 + \mu_2^{\text{sac}}/\varepsilon_2 + \mu_3^{\text{LMC-2}}/\varepsilon_3 = 0.11\,\text{D} \quad (7)$$

From the above equations, we obtained $\mu_3^{\text{LMC-1}} = 0.69$ D, $\mu_3^{\text{LMC-1-H}} = 0.38$ D, and $\mu_3^{\text{LMC-2}} = 0.22$ D.

Finally, to make sure the suitability of the above set of parameters, we rechecked the contribution of the polar head group to the dipole moment for DPPC and DPPE. We have

Table 2
Surface potential data used for dipole moment evaluation

Sample	A_0 (nm^2)	ΔV (mV)
Stearic acid	0.20	313
PA-0-5	0.49	316
LMC-1	0.42	249
LMC-1-H	0.32	197
LMC-2	0.39	104
DPPC	0.43	527
DPPE	0.38	589

A_0 is the molecular surface area obtained by extrapolating the high-pressure portion of the π–A isotherms to zero pressure. ΔV is the surface potential at maximum compression. In all cases, the subphase was 0.5 M NaCl at 298.2 K.

used the CH_3 group of $2 \times 0.33\,D = 0.66\,D$ for the following equations:

$$\mu_\perp(\mathrm{DPPC}) = \mu_1/\varepsilon_1 + \mu_2^{\mathrm{PC}}/\varepsilon_2 + \mu_3^{\mathrm{CH3}}/\varepsilon_3 = 0.60\,D \quad (8)$$

$$\mu_\perp(\mathrm{DPPE}) = \mu_1/\varepsilon_1 + \mu_2^{\mathrm{PE}}/\varepsilon_2 + \mu_3^{\mathrm{CH3}}/\varepsilon_3 = 0.59\,D \quad (9)$$

The above two equations allowed us to obtain $\mu_2^{\mathrm{PC}} = 2.75\,D$ for PC head and $\mu_2^{\mathrm{PE}} = 2.68\,D$ for PE head. These values are a little bit larger than those resported by Taylor et al. for DPPC and DPPE (2.44 and 2.23 D, respectively) [33]. In each case, the difference in ΔV may result from a change in PC and PE hydration. Also, the $\mu_\perp$ values for PC and PE must reflect the water structure. Then, these differences may result from variation in experimental conditions such as substrate composition (electrolyte, pH), compression rate, and so forth.

3.3. Compression isotherms of cerebrosides/phospholipids two-component monolayers

Next, turning to the discussion toward two-component systems, four combinations of two-component monolayer systems composed of the two cerebrosides (LMC-1 and LMC-2) and two phospholipids (DPPC and DPPE) have been studied in order to clarify the effect of molecular structure, the interaction between two components, and the miscibility on the monolayer state. For the above purpose, the π–A, ΔV–A, and $\mu_\perp$–A isotherms were measured at various compositions at 298.2 K on a 0.5 M NaCl subphase for LMC-1/DPPC and LMC-2/DPPC and DPPE two-component systems of the four combinations. The isotherms of four two-component systems are shown in Fig. 3. The isotherms of five two-component at discrete mole fractions are also inserted in the corresponding figures. All the curves of the two-component systems exist between those of the respective pure components, and they successively change with the increasing mole fraction of phospholipids.

3.3.1. Cerebrosides (LMC-1 and LMC-2)/DPPC systems

The π–A isotherms of two-component monolayers for the cerebrosides (LMC-1 and LMC-2) and DPPC systems are shown in Fig. 3A and B. Increasing amounts of the cerebrosides does not result in a clearly distinguishable phase transition from liquid-expanded to liquid-condensed phase. The change and disappearance of such transition pressure with increasing amounts of the cerebrosides suggest that cerebrosides have an ability to make DPPC miscible in the monolayers, which is mentioned in the later section of two-dimensional phase diagram. This observation is a first evidence of the miscibility for the two components within the monolayer. As it is difficult to ascertain the presence of the transition pressure at the mole fractions <0.3 on the π–A isotherms, we have investigated cerebrosides/phospholipids two-component monolayers by fluorescence microscopy (later section).

The interaction between LMC-1 or LMC-2 and DPPC molecules was investigated by examining whether the variation of the mean molecular areas as a function of X_{DPPC} satisfies the additivity rule [37]. Comparison between the experimental mean molecular areas and the mean molecular areas based on ideal mixing is shown in Fig. 4A and B at four surface pressures (5, 15, 25, and 35 mN m^{-1}). For $\pi = 5$ mN m^{-1} of LMC-1/DPPC system (Fig. 4A), experimental values show a negative deviation from the theoretical line, indicating attractive interaction between LMC-1 and DPPC. This may result from the fact that the interactions between LMC-1 and DPPC are mainly governed by the enhanced attractions between hydrophobic groups. For $\pi = 15$ and 25 mN m^{-1} of LMC-1/DPPC system, positive deviations are observed, indicating diminished interaction between the head groups of LMC-1 and DPPC and between fatty acid chains of LMC-1 and DPPC. At 35 mN m^{-1}, the variation almost obeys the additivity rule. This indicates that LMC-1 and DPPC are almost ideally mixed in the monolayer. As LMC-1 has a longer alkyl chain than DPPC, attractive interaction between LMC-1 hydrocarbon segments and DPPC chains is maximized and compensates for steric hindrance produced by the LMC-1 hydrocarbon segment. For LMC-2/DPPC system (Fig. 4B), comparison of the experimental data with calculated values clearly indicates a good agreement at 5 and 35 mN m^{-1}. The A–X_{DPPC} shows positive deviations at 15 and 25 mN m^{-1}. These behaviors are explained as the same of LMC-1/DPPC system.

The influence of X_{DPPC} on the ΔV–A and $\mu_\perp$–A isotherms is shown in Fig. 3A and B. Analysis of the surface potential (ΔV) of the two-component monolayers in terms of the additivity rule is presented in Fig. 5A and B. For LMC-1/DPPC system (Fig. 5A), comparison of the experimental data versus calculated variations clearly indicates a good agreement with the ideal line at 5 mN m^{-1} and negative deviations at 15–35 mN m^{-1}. On the other hand, the ΔV–X_{DPPC} of LMC-2/DPPC system (Fig. 5B) shows slightly positive deviation at 5 mN m^{-1} and the good agreement at 15–35 mN m^{-1}.

3.3.1.1. Mean surface areas (A_m), partial molecular surface areas (PMA), mean surface potentials (ΔV_m), and apparent partial molecular surface potentials (APSP).

When π–A isotherms of a given binary mixture are analyzed, it is essential to examine whether the relation of mean surface area (A_{m}) with mole fraction (X) satisfies the additivity rule or not, and if not, which deviation is observed, negative or positive.

In Fig. 4A and B, the A_{m} for the LMC-1/DPPC and LMC-2/DPPC two-component systems is plotted against X_{DPPC} at discrete surface pressure of 5, 15, 25, and 35 mN m^{-1}. A binary system can show an ideal behavior by either (1) forming ideally mixed monolayer or (2) the two components cannot mix completely but can form the so-called patched film, where the additivity should show a linear relation as indicated by a broken line.

The behavior of occupied surface area and surface potential can be seen more clearly if the partial molar quantities are evaluated, where one of them have been employed in previous studies [38,39]. Here A_{m} and ΔV_{m} are assumed to satisfy

the following equations: the additivity rule for mean surface area can be expressed as

$$A_{\mathrm{m}} = X_1 A_1 + X_2 A_2$$

where A_{m} is the average molecular area in the two-component film, X_1 and X_2 are the mole fractions of the components 1 and 2, respectively, and A_1 and A_2 are the partial molecular areas (PMA) in the two-component film at a definite surface pressure. Correspondingly, the surface potential should be given by

$$\Delta V_{\mathrm{m}} = X_1 \Delta V_1 + X_2 \Delta V_2$$

where ΔV_{m} is the average molecular surface potential in the two-component film, and ΔV_1 and ΔV_2 are the partial molecular surface potential in the two-component film at a definite surface pressure. When PMA is denoted as A_1 and A_2 for components 1 and 2, the A_1 and A_2 values can be determinable as the respective intercept value at $X_2 = 0$ and $X_2 = 1$ of a tangential line drawn at any given point on the A_{m}–$X_{\mathrm{phospholipid}}$

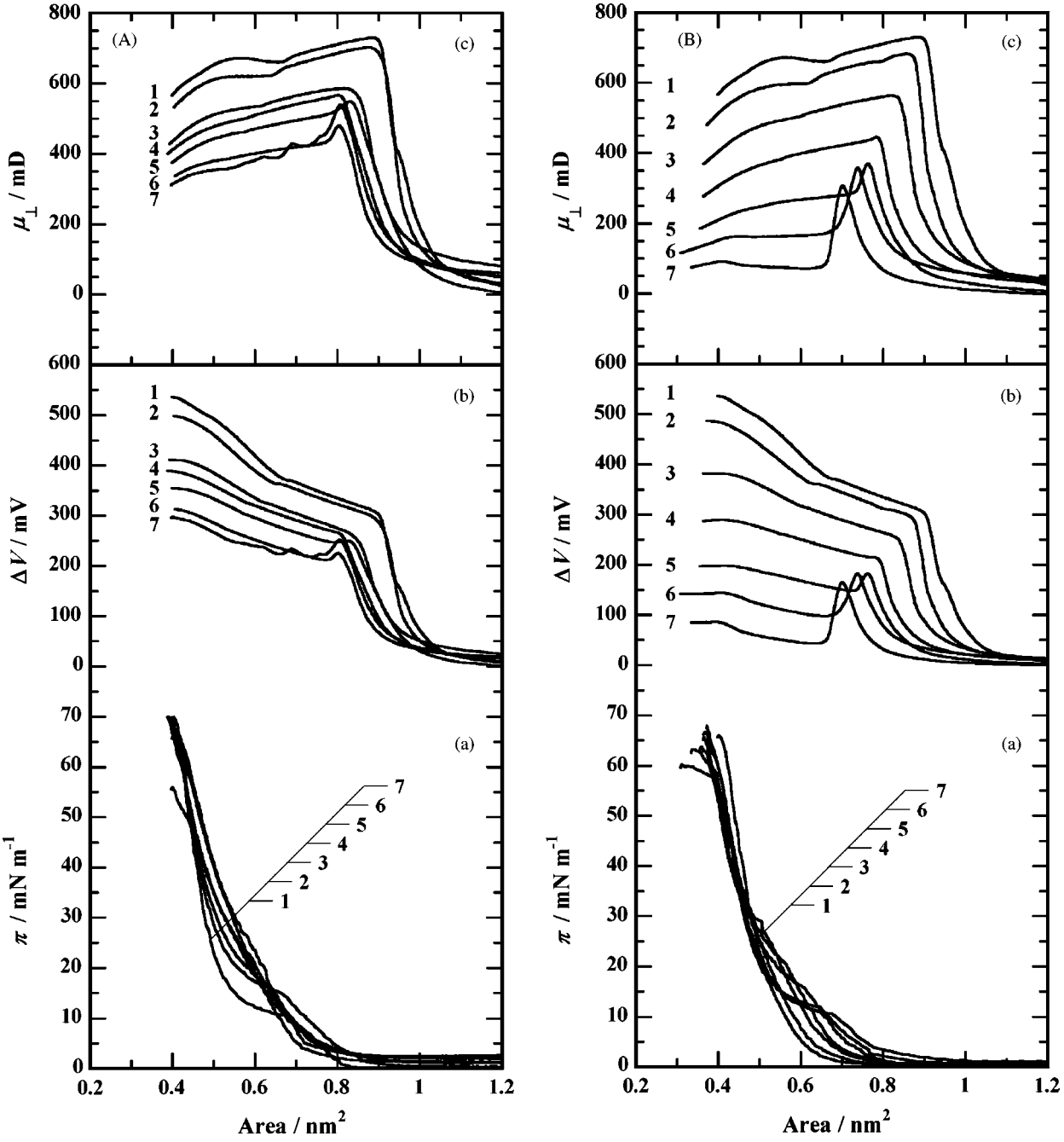

Fig. 3. Surface pressure (π)–area (A) isotherms, surface potential (ΔV)–A isotherms, and surface dipole moment ($\mu_\perp$)–A isotherms of the two-component systems on 0.5 M NaCl at 298.2 K: (A) LMC-1/DPPC, (B) LMC-2/DPPC, (C) LMC-1/DPPE, and (D) LMC-2/DPPE systems.

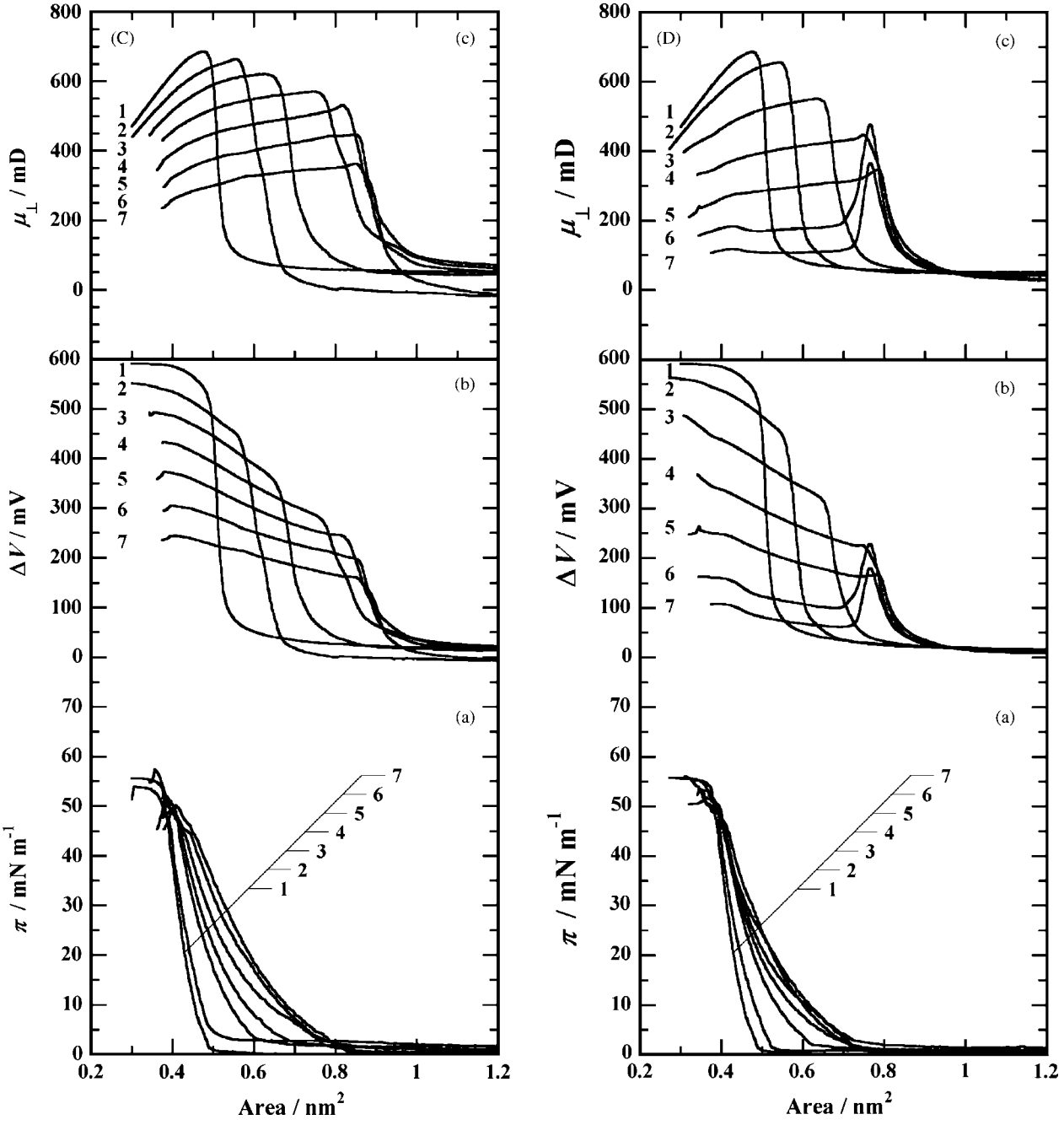

Fig. 3. (*Continued*).

curve as shown in Fig. 4. A_1 and A_2 from the relation are given as

$$A_1 = A_m - X_2\left(\frac{\partial A_m}{\partial X_2}\right)_{T,\pi} \quad (10)$$

$$A_2 = A_m + (1 - X_2)\left(\frac{\partial A_m}{\partial X_2}\right)_{T,\pi} \quad (10')$$

where A_i is defined as

$$A_i = \left(\frac{\partial A_i}{\partial N_i}\right)_{T,\pi}$$

when N_1 plus N_2 molecules form a surface area A_t ($=N_1A_1 + N_2A_2$), and 1 and 2 denote cerebrosides and DPPC, respectively. Correspondingly, the apparent partial molecular surface potential (APSP) can be obtained from the relationship between the average molecular surface potential and mole fraction, which is the same as above area

$$\Delta V_1 = \Delta V_m - X_2\left(\frac{\partial \Delta V_m}{\partial X_2}\right)_{T,\pi} \quad (11)$$

where ΔV_m was evaluated by dividing the measured surface potential (ΔV) by the number of molecules in the unit area.

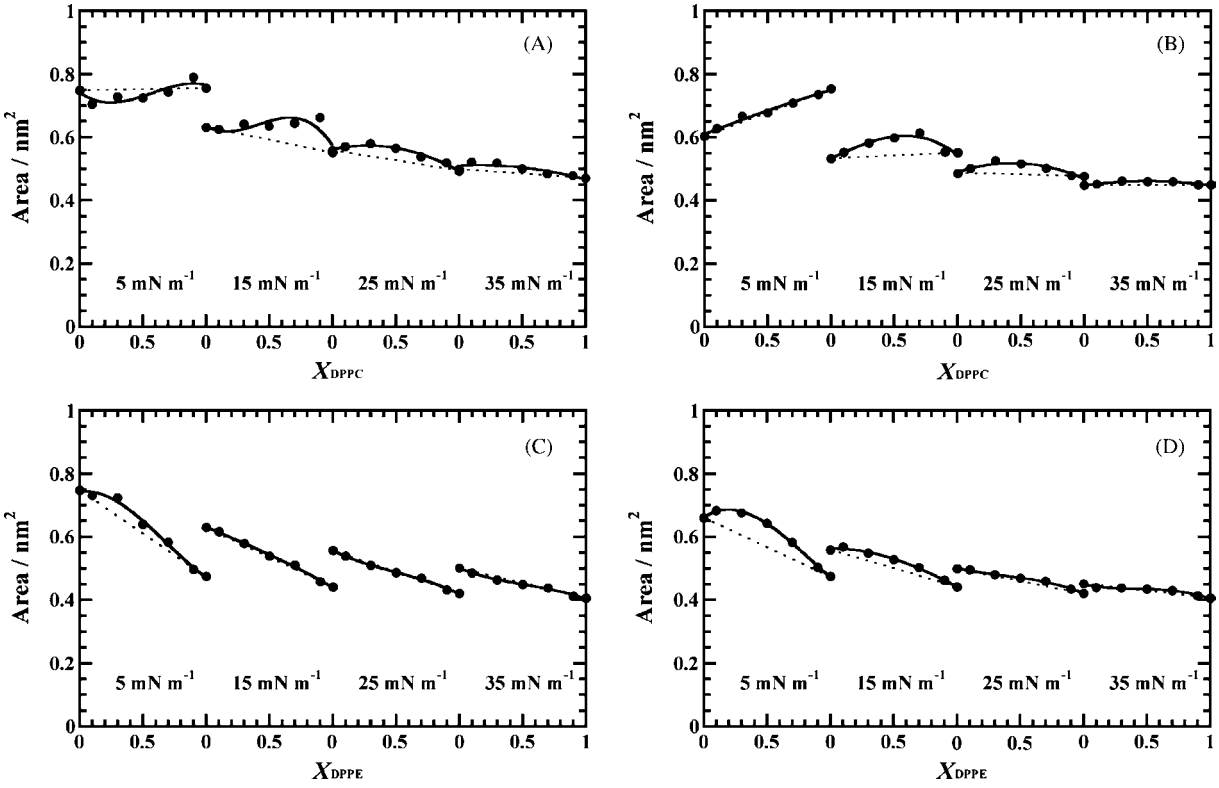

Fig. 4. Deviation of two-component monolayer behavior from ideal one. Variation of the mean molecular area with phospholipid mole fraction for the cerebrosides/phospholipids mixtures at surface pressures of 5, 15, 25, and 35 mN m^{-1}: (A) LMC-1/DPPC, (B) LMC-2/DPPC, (C) LMC-1/DPPE, and (D) LMC-2/DPPE systems.

The surface potential (ΔV) is measured by an air electrode whose area is ca. 1 cm^2. Therefore, we assumed its dimension to be by mV cm^{-2}. The average molecular surface potential (ΔV_m) in mV molecule^{-1} unit can be obtained by the ΔV and the number of molecules in 1 cm^2 calculated from the π–A isotherm. When APSP is denoted as ΔV_1 and ΔV_2 for components 1 and 2, they are determined by the respective intercepts at $X_2 = 0$ and $X_2 = 1$ of a tangential line drawn at any given point on the ΔV_m–$X_{phospholipid}$ curve as shown in Fig. 6.

For cerebrosides/DPPC systems, they were miscible due to the evidence of transition pressure change behavior which increases with X_{DPPC} (mentioned above). So, PMA and APSP procedures were applied to cerebrosides/DPPC systems. The PMA–X_{DPPC} curves for cerebrosides/DPPC systems are shown in Fig. 7. It is noted that if the two-component systems are ideal mixing, PMA and APSP should be parallel to the axis of X_2 (the additivity rule). The PMA for both cerebrosides/DPPC systems indicates the similar behavior at each surface pressure except for low surface pressure of 5 mN m^{-1}. It is found that DPPC molecules have almost same surface area in the binary LMC-1 or LMC-2/DPPC systems. At 5 mN m^{-1} of LMC-1/DPPC system, the partial molecular areas of LMC-1 and DPPC do not remain constant over the whole mole fraction. On the contrary, as for LMC-2/DPPC system, those of LMC-2 and DPPC show individual one over the whole mole fraction. At 15 mN m^{-1} of cerebrosides/DPPC systems, the partial molecular areas of both systems are very changeable too. This complex behavior comes from the LE/LC transition of DPPC. The characteristic PMA behavior may be directly related to the liquid-expanded state of DPPC. At the higher surface pressure (35 mN m^{-1}), where DPPC molecules form a liquid-condensed film, all molecular areas of the two mixtures show an almost linear in regard to A_m versus X_{DPPC} plots, although small positive deviations from the additivity rule are seen. However, these deviations are not attributable to experimental errors.

In contrast to PMA, the APSP–X_{DPPC} curves for cerebrosides/DPPC systems (see Fig. 8) suggest the different interaction of DPPC between LMC-1 and LMC-2. The APSP–X_{DPPC} for LMC-1/DPPC systems indicates the similar behavior at each surface pressure. It is found that APSP of DPPC and LMC-1 molecules remain almost the same as the individual value over the whole mole fraction range as shown in Fig. 8A. Those of DPPC and LMC-2 are shown in Fig. 8B. Upon compression at 5 and 15 mN m^{-1}, APSP of DPPC decreases with increasing mole fraction of DPPC, and the value reaches the original value. For example, DPPC molecules at $X_{DPPC} = 0.1$ are surrounded almost by the LMC-2 molecules for the binary LMC-2/DPPC system. In the monolayer, DPPC has a minimum molecular area of about 0.46 nm^2 (Fig. 1) [40,41], which is limited by the relatively large head group cross-sectional area. The cross-sectional area of an optimally packed, all *trans*, hydrocarbon chain is about 0.20 nm^2 [42],

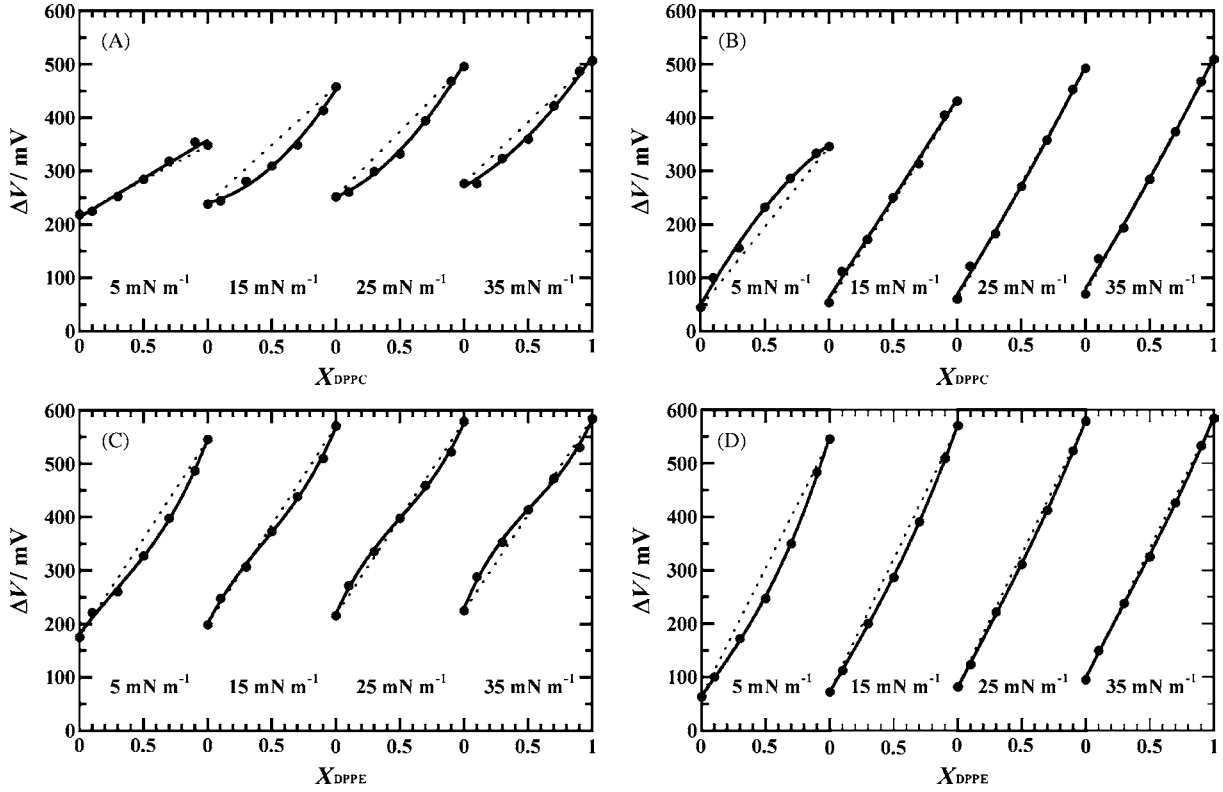

Fig. 5. Deviation of two-component monolayer behavior from ideal behavior. Variation of the surface potential with phospholipid mole fraction for the cerebrosides/phospholipids mixtures at surface pressures of 5, 15, 25, and 35 mN m^{-1}: (A) LMC-1/DPPC, (B) LMC-2/DPPC, (C) LMC-1/DPPE, and (D) LMC-2/DPPE systems.

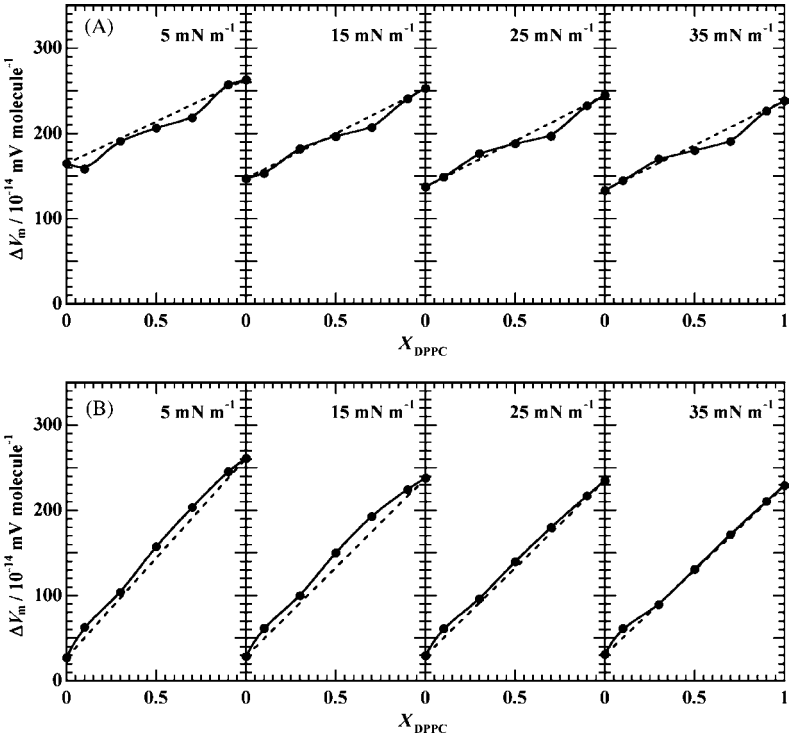

Fig. 6. Variation of the mean molecular surface potential (ΔV_m) with phospholipid mole fraction for the cerebrosides/DPPC mixtures at surface pressures of 5, 15, 25, and 35 mN m^{-1}: (A) LMC-1/DPPC, (B) LMC-2/DPPC.

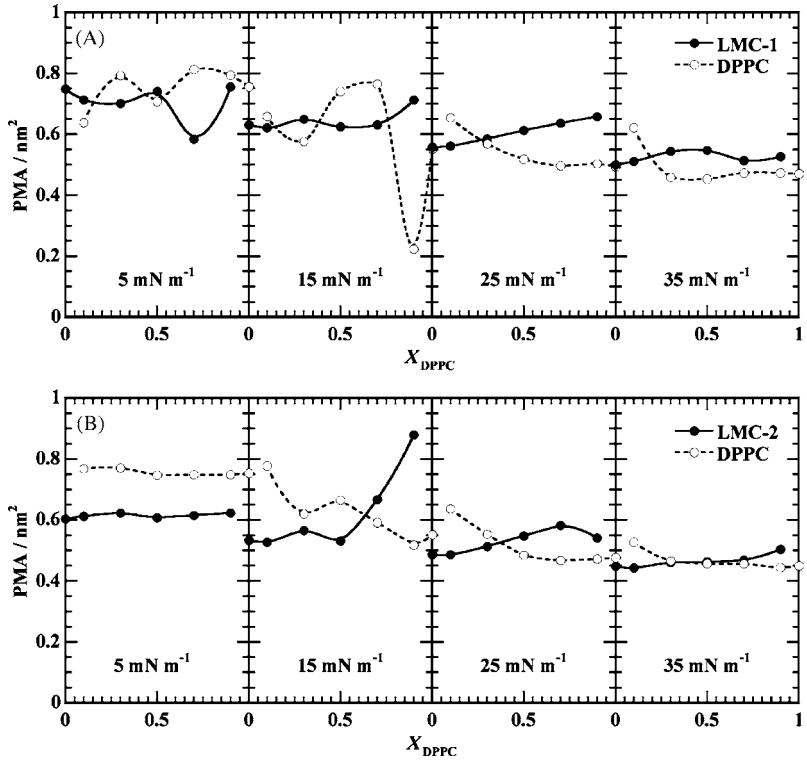

Fig. 7. Variation of partial molecular surface area (PMA) for two-component cerebrosides and DPPC as a function of X_{DPPC} at surface pressures of 5, 15, 25, and 35 mN m^{-1}: (A) LMC-1/DPPC and (B) LMC-2/DPPC systems.

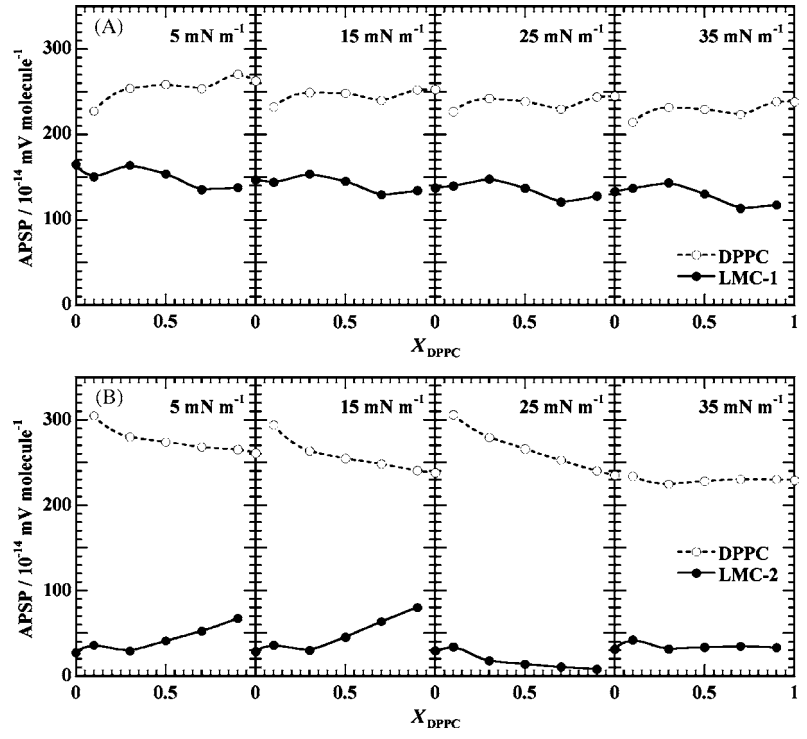

Fig. 8. Variation of apparent partial molecular surface potential (APSP) for two-component cerebrosides and DPPC as a function of X_{DPPC} at surface pressures of 5, 15, 25, and 35 mN m^{-1}: (A) LMC-1/DPPC and (B) LMC-2/DPPC systems.

so the hydrocarbon portion of the DPPC molecule would like to occupy an area of $A = 2\,\text{nm} \times 0.20\,\text{nm} = 0.40\,\text{nm}^2$. This mismatch results in a tilt angle of aliphatic chains of 25–30° and a reduction in the attractive interactions between the chains [40,43]. Tilting is also accompanied by a decrease in the coherence length of monolayer packing.

Addition of LMC-2 reduces the head/tail mismatch of pure DPPC as shown by potential increase of APSP for DPPC, indicating the decrease in tilt angle of the mixed monolayer state. Increasing the mole fraction of DPPC increases the APSP of LMC-2 at lower surface pressures, leading to a good conformation with DPPC. Upon compression at 25 mN m^{-1}, for mole fraction of 0.1 and 0.3, part of DPPC changes to LC film via transition pressure π^{eq}. APSP for DPPC indicates the decrease in tilt angle of the mixed monolayer state at the sacrifice of orientation for LMC-2.

Upon compression at 35 mN m^{-1}, APSP behavior of both DPPC and LMC-2 are parallel to the axis of X_{DPPC}. The APSP for both DPPC and LMC-2 has the individual value at each mole fraction owing to high surface pressure.

For the LMC-1/DPPC system, both components show almost the individual values over the whole mole fraction, resulting from matching of DPPC chains (saturated) and LMC-1 ones (unsaturated). On the other hand, the packing for the LMC-2/DPPC system changes depending upon the surface pressure. This behavior is owing to the matching of the chain length of DPPC (saturated) and to the position of OH group in LMC-2 chains (saturated). In consequence, the surface orientation of DPPC molecules are affected more strongly by LMC-2 chains than LMC-1 ones due to the position of OH group in LMC-2 chains (saturated).

3.3.2. Cerebrosides (LMC-1 and LMC-2)/DPPE systems

Fig. 3C and D shows π–A, ΔV–A, and $\mu_\perp$–A isotherms of binary LMC-1/DPPE and LMC-2/DPPE systems, respectively. Both cerebrosides and DPPE had no transition points on their π–A isotherms. In addition, the π–A isotherms and fluorescence images (later section) indicated the LE film for cerebrosides and LC film for DPPE.

The interaction between LMC-1 or LMC-2 and DPPE molecules was analyzed in the same procedures as the Section 3.3.1 (for additivity rule of area and ΔV). The A–X_{DPPE} (Fig. 4C) shows a positive deviation at 5 mN m^{-1} and good agreements with the ideal line at 15–35 mN m^{-1}, while it (Fig. 4D) does positive deviations at 5–15 mN m^{-1} and the good agreements at 25–35 mN m^{-1}. For ΔV–X_{DPPE} in Fig. 5C and D, both LMC-1/DPPE and LMC-2/DPPE systems indicate negative deviations at 5 mN m^{-1} and the good agreements at 15–35 mN m^{-1}. These behaviors can be explained by the above-mentioned interpretation.

3.4. Two-dimensional phase diagram

From the π–A isotherm for the binary systems of LMC-1/DPPC, LMC-2/DPPC, LMC-1/DPPE, and LMC-2/DPPE, their two-dimensional phase diagrams were constructed by use of the transition pressure (π^{eq}) and/or the collapse pressure (π^c) changes at various mole fractions of phospholipids. Representative phase diagrams at 298.2 K are shown in Fig. 9.

3.4.1. Cerebrosides/DPPC

The transition pressures from disordered (gaseous or liquid-expanded) to ordered (liquid-condensed) phase are also plotted against a mole fraction of phospholipid in Fig. 9A and B. In LMC-1/DPPC and LMC-2/DPPC systems for $X_{DPPC} = 0.3$ to 1, π–A isotherm displays a phase transition pressure (π^{eq}) that changes almost linearly with X_{DPPC}. Judging from the change of the transition pressure, two components of all other mole fractions are miscible each other. This behavior is a first evidence of the miscibility of the two components within the monolayer state. This can be explained by the fact that film-forming molecules become more dense by compression, decreasing the surface tension more by the film-forming molecule. Then the resultant surface pressure increased. Decrease in the transition pressure with mole fraction of DPPC means that transition does appear when the film-forming molecules become denser with the mole fraction. These phenomena resemble the elevation of boiling point and the depression of freezing point in the mixed solution.

Assuming that in these cerebrosides/DPPC cases the surface mixtures behave as a regular solution with a hexagonal lattice, the coexistence phase boundary between the ordered monolayer phase and the bulk phase can be theoretically simulated by the Joos equation (12), and the interaction parameter (ξ) was calculated from this deviation [44]:

$$1 = x_1^s \gamma^1 \exp\{(\pi_m^c - \pi_1^c)\omega_1/kT\}\exp\{\xi(x_2^s)^2\} + x_2^s \gamma^2 \exp\{(\pi_m^c - \pi_2^c)\omega_2/kT\}\exp\{\xi(x_1^s)^2\} \quad (12)$$

where x_1^s and x_2^s denote the mole fraction in the two-component monolayer of components 1 and 2, respectively, and π_1^c and π_2^c are the corresponding collapse pressures of components 1 and 2. π_m^c is the collapse pressure of the two-component monolayer at given composition of x_1^s and x_2^s. ω_1 and ω_2 are the corresponding limiting molecular surface area at the collapse points. γ^1 and γ^2 are the surface activity coefficients at the collapse point, ξ is the interaction parameter, and kT is the product of the Boltzmann constant and the Kelvin temperature.

In these figures, **M.** indicates a two-component monolayer formed by cerebroside and DPPC species, while **Bulk** denotes a solid phase of cerebrosides and DPPC ("bulk phase" may be called "solid phase"). The collapse pressure π^c determined at each mole fraction is indicated by filled circles, where the dotted line shows the case where the interaction parameter (ξ) is zero.

From this equation, the interaction parameter ξ is obtained, and these mixtures yield $\xi = -1.50$ (for LMC-1/DPPC) and -0.10 (for LMC-2/DPPC). This means that there is mutual interaction between two components in the two-component monolayer that is stronger than the mean of the interactions

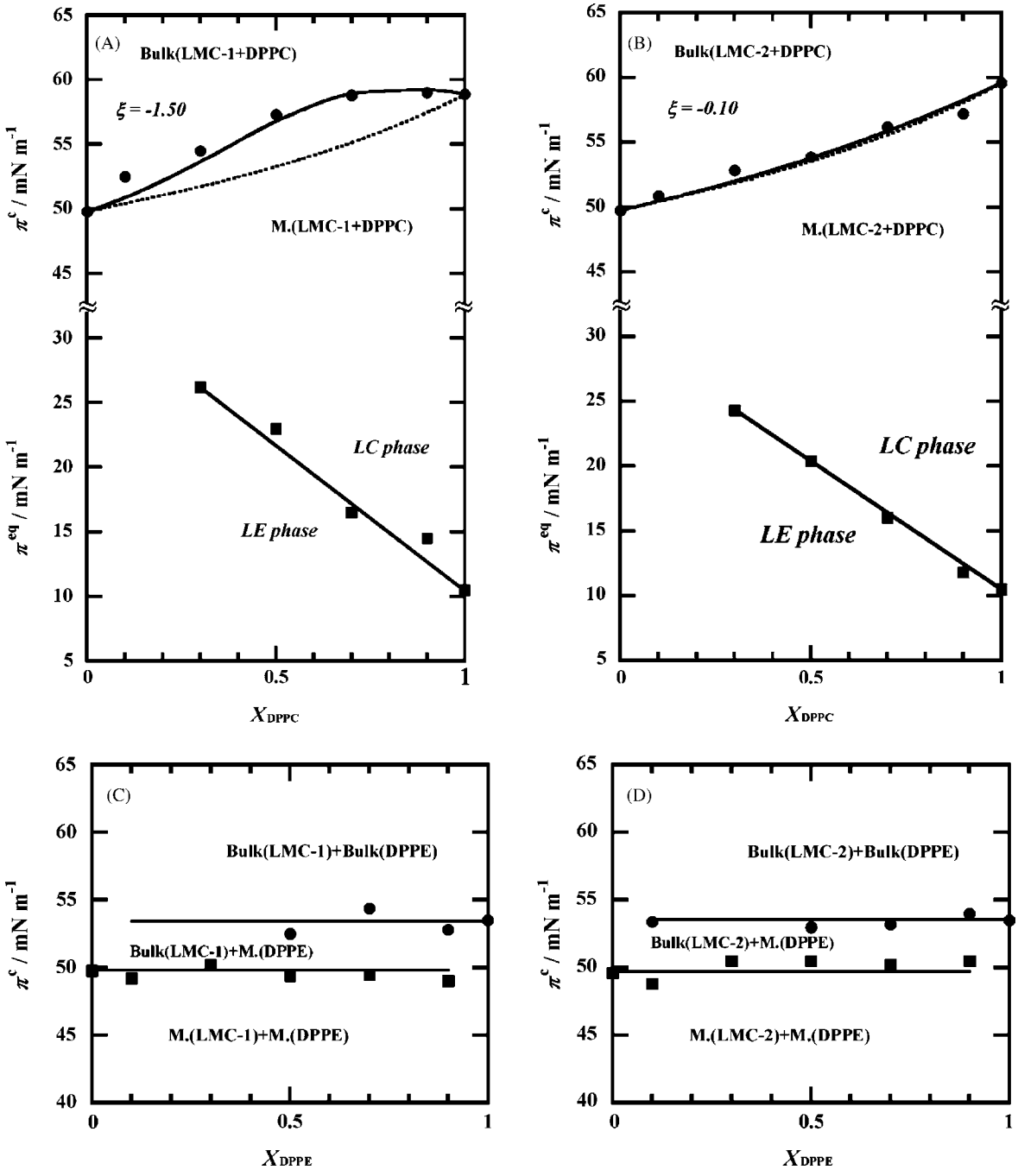

Fig. 9. Change of the transition pressure (π^{eq}) and the collapse pressure (π^{c}) as a function of $X_{phospholipid}$ on 0.5 M NaCl at 298.2 K. The dashed line was calculated by Eq. (12) for $\xi = 0$: (A) LMC-1/DPPC, (B) LMC-2/DPPC, (C) LMC-1/DPPE, and (D) LMC-2/DPPE systems.

between pure component molecules themselves. As a result, they are completely mixing. The interaction energy $-\Delta\varepsilon$ can be calculated the following equation:

$$-\Delta\varepsilon = -\xi RT/6 \tag{13}$$

and these values are $620\,J\,mol^{-1}$ (for LMC-1/DPPC) and $41\,J\,mol^{-1}$ (for LMC-2/DPPC). As a result, cerebrosides/DPPC systems are the positive azeotropic type.

3.4.2. Cerebrosides/DPPE

Next, the second type of phase diagram is constructed in Fig. 9C for LMC-1/DPPE and Fig. 9D for LMC-2/DPPE, which are same procedures as the above cases. We recognized that DPPE is completely immiscible with cerebrosides. For example, in the phase diagrams for LMC-1/DPPE at lower π values, LE film of cerebroside (LMC-1) is formed independent upon a DPPE; the film is separated into LMC-1 domains and DPPE domains, like island and sea. Their region is ex-

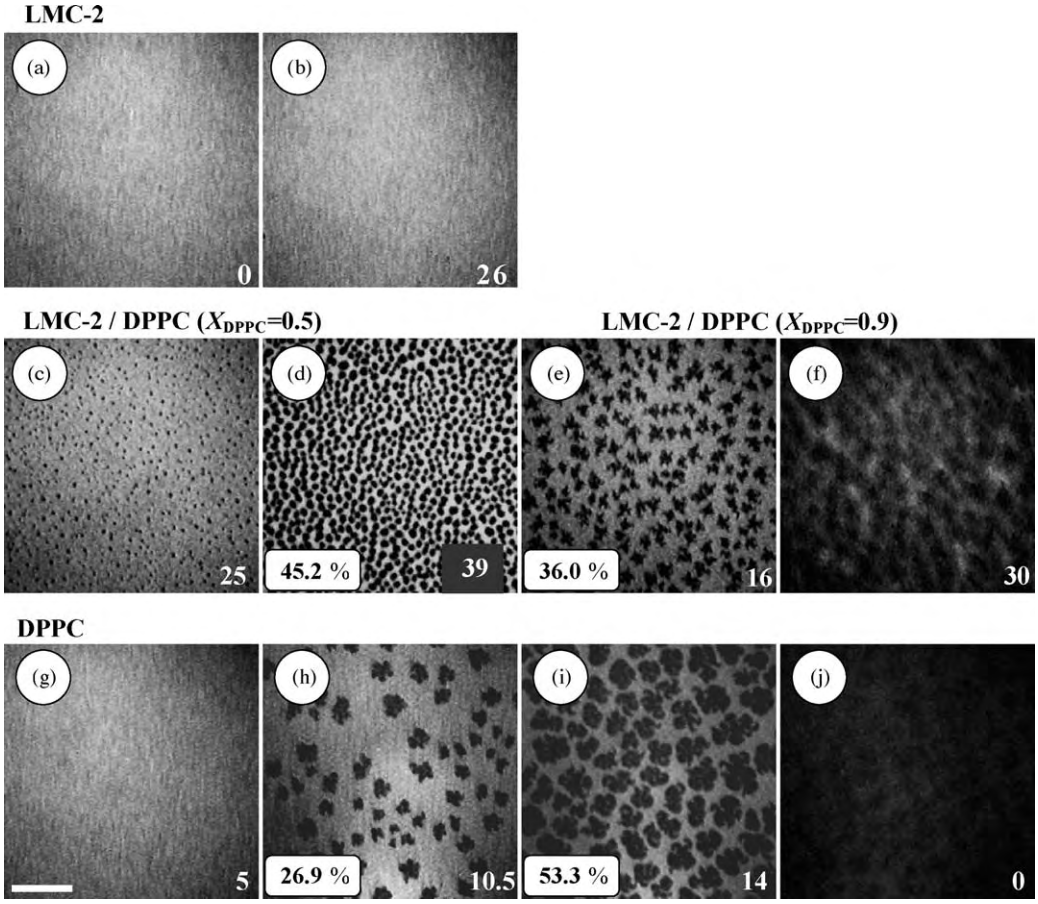

Fig. 10. Fluorescence micrographs of LMC-2 monolayer (a: 0, b: 26 mN m^{-1}), LMC-2/DPPC two-component monolayer (X_{DPPC} = 0.5) (c: 25, d: 39 mN m^{-1}), LMC-2/DPPC two-component monolayer (X_{DPPC} = 0.9) (e: 16, f: 30 mN m^{-1}) and DPPC monolayer (g: 5 mN m^{-1}, h: 10.5 mN m^{-1}, i: 14 mN m^{-1}, j: 30 mN m^{-1}) observed at a compression rate of 1.0×10^{-1} nm^2 molecule^{-1} min^{-1} at 298.2 K on 0.5 M NaCl. The monolayer contained 1 mol% of fluorescent probe. The number in these images indicates the surface pressure (mN/m). Scale bar represents 50 μm.

pressed as M.(LMC-1) + M.(DPPE). If further compression of the film is made up to the collapse pressure of the given LMC-1, then the LMC-1 starts to form a solid (Bulk) of its own (denoted Bulk(LMC-1) in the figure). Until the LMC-1 completes its solid formation, the surface pressure is kept constant. At much higher pressure of π, bulks of LMC-1 and DPPE coexist independently, as shown by Bulk(LMC-1) + Bulk(DPPE). In the middle surface pressure region, the monolayer (LC) of DPPE coexists with bulk state of the given LMC-1.

The above implies that cerebrosides and DPPE cannot mix in the monolayer state. This means that the lateral steric interaction between cerebrosides and DPPE is extremely unfavorable. Then, two components are completely separated, and they form patched monolayers. Therefore, this phase diagram is divided into three parts by double parallel lines.

3.5. Fluorescence microscopy of cerebrosides/phospholipids two-component monolayers

In order to interpret the phase behavior on the π–A isotherms, we investigated the monolayers by fluorescence microscopy, which provides a direct image of the monolayers. A fluorescent dye probe was therefore incorporated into the monolayer and its distribution was monitored by fluorescence micrographs. The contrast is due to difference in dye solubility between disordered (or LE) and ordered phases (or LC). Representative fluorescence micrographs (FMs) of pure LMC-2, DPPC, DPPE, and their two-component monolayers spread on 0.5 M NaCl at 298.2 K are shown in Figs. 10 and 11 at various surface pressures.

3.5.1. Cerebroside (LMC-2)/DPPC

Before examining the effects of a cerebroside on DPPC domain shape, it is necessary to make pure DPPC behavior clear. The π–A isotherm of DPPC is shown in Fig. 2B, where there exists the LE/LC coexistence region. Domain nucleation occurs at the kink in the π–A isotherm (typically at 10.5 mN m^{-1}). Initially, the domains appear roughly round in shape: whether the shape is the case in reality or due to limits in the resolution of the microscope is unclear. Indeed, only when they grow, they take their fundamental shape in Fig. 10.

Fig. 10g–j shows a progression of fluorescence images through the coexistence region for DPPC [45–47]. The nu-

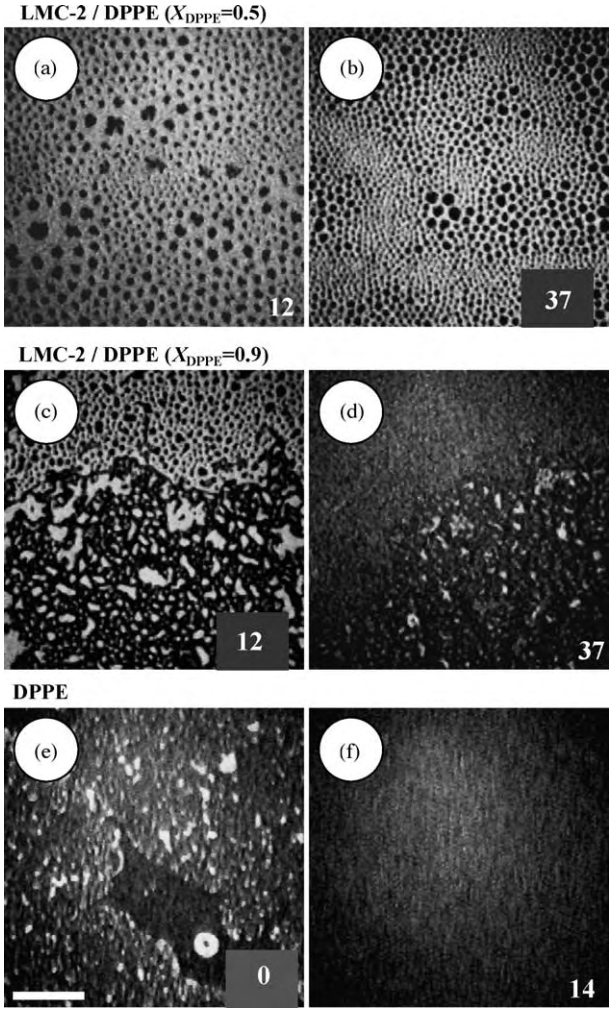

Fig. 11. Fluorescence micrographs of LMC-2/DPPE two-component monolayer (X_{DPPE} = 0.5) (a: 12 mN m^{-1}, b: 37 mN m^{-1}), LMC-2/DPPE two-component monolayer (X_{DPPE} = 0.9) (c: 12 mN m^{-1}, d: 37 mN m^{-1}) and DPPE monolayer (e: 0 mN m^{-1}, f: 14 mN m^{-1}) observed at a compression rate of 1.0×10^{-1} nm^2 molecule^{-1} min^{-1} at 298.2 K on 0.5 M NaCl. The monolayer contained 1 mol% of fluorescent probe. The number in these images indicates the surface pressure (mN/m). Scale bar represents 50 μm.

merical value shows surface pressure in the figures and the percentage is ratio of LC domain in each image to the total area. They indicate the gaseous phase at 5 mN m^{-1} and the coexistence state of both LE phase and LC phase at 10.5 and 14 mN m^{-1}, where the bright regions and dark domains indicate LE and LC phase, respectively. With increasing surface pressure from 10.5 to 14 mN m^{-1}, the percentage of LC phase in each image increases and complete LC domain image appears at 20 mN m^{-1} (data not shown). The domains formed are chiral, which is an expression of the chirality of the DPPC molecule. As would be expected, the enantiomer forms mirror images of the domains, and a racemic mixture yields nonchiral domains. As is most evident in Fig. 10h at 10.5 mN m^{-1}, the predominant domain shape is like a bean with distinct cavities. As the monolayer is compressed, the domains grow and display their repulsive nature (arising from their oriented dipoles) by deforming themselves to fill all available space and transforming into polygons. At the surface pressures between 11 and 15 mN m^{-1}, there happens a shape instability resulting in 'cutting' the domain along intrinsic chiral paths as shown in Fig. 10i at 14 mN m^{-1}. This phase transition is attributed to the presence of the fluorescence probe, because no such effect is seen by Brewster angle microscopy [46]. In addition, the phase transition is completely suppressed at higher compression rates, suggesting a kinetic rather than a thermodynamic origin.

Monolayers of cerebroside used in this study do not form the LC domains in the monolayer. As a result, FM shows the liquid-expanded image (Fig. 10a and b). As mentioned in Section 2, cerebrosides were molecular species and the hydrophobic parts of LMC-2 are too bulky to be closely packed together compared with their occupied area of the polar head group. A cavity is formed among the hydrocarbon parts of LMC-2 because of the molecular structure. The white patterns in the FM image are the evidence of such LE domains independence of surface pressure (Fig. 10a and b).

Next, the mole fraction dependence of the transition pressure is observed on the FM images of the two-component system of LMC-2/DPPC in Fig. 10c and d for X_{DPPC} = 0.5, and Fig. 10e and f for X_{DPPC} = 0.9. At low surface pressures ($\pi < \pi^{eq}$), cerebroside/DPPC systems of two-component monolayer were uniformly fluoresced, showing apparently homogeneous LE phase without liquid-condensed (LC) phase of dark domains. Increasing the surface pressure, LC domains appear at X_{DPPC} = 0.5 and 0.9. In each case, the LE/LC coexistence region is observed and transition pressure (π^{eq}) is higher than that of pure DPPC (Figs. 9B, and 10c and e). This suggests that the observed dark domains in these figures would represent a condensed DPPC-enriched phase. With increasing the surface pressure, the conformation change of the polar head groups in the two-component monolayer is to facilitate the formation of the small LC domains of DPPC. The increment in concentration of cerebroside (at X_{DPPC} = 0.5) makes the LE phase image larger, and the dark domains of DPPC became small (Fig. 10c). In this system, the LC domains were distributed homogeneous and observed to undergo the Brownian motion in the monolayer. At high surface pressure, the growth of circular LC domains persisted in cerebroside/DPPC two-component monolayers. As a result, this system is completely miscible each other.

3.5.2. Cerebroside (LMC-2)/DPPE

Fluorescence images of LMC-2/DPPE monolayers on 0.5 M NaCl solution are shown in Fig. 11. The pure DPPE monolayer showed some large domains at very low surface pressure (Fig. 11e). The fluorescent probe of R18 (1 mol%) partitions into the disordered LE phase in preference to the better ordered LC phase. However, the fluorescence of R18 is quenched by contact with water [48,49], and the dark black regions at low surface pressure are the gaseous phase owing to complete quenching of the fluorescence. The intermediate

gray regions are the LC phase, and the bright regions are the disordered phase. Film compression results in the formation of the LC phase from the disordered phase, and these fluorescence images became completely black above the surface pressure of 5 mN m^{-1}. In contrast, the images of pure LMC-2 showed no indication of lateral phase separation regardless of surface pressure (π), showing the liquid-expanded behavior (i.e. the whole images were bright).

Fig. 11a–d shows the LMC-2/DPPE two-component monolayer at the mole fractions $X_{DPPE} = 0.5$ and 0.9, respectively. The addition of some amounts of DPPE to LMC-2 induced the ordered/disordered phase separation at zero surface pressure. Changes of morphologies of this phase separation do not take place up to high surface pressure. This suggests that LMC-2 has a dispersing effect for DPPE. However, according to the mentioning in the earlier section, LMC-1 and LMC-2 showed miscibility with the DPPC. Therefore, it turned out that the miscibility of LMC-2 with DPPC or DPPE can be attributed to the difference of the polar head group. Fluorescence microscopy for DPPE/LMC-2 system showed that LMC-2 escapes from the entirely condensed solid phospholipid domains with increasing mole fraction of LMC-2, while the LMC-2 disperses the condensed domains heterogeneously. This indicates that the LMC-2 acts as the dispersing agent for the condensed phospholipid.

4. Conclusion

The cerebrosides derived from echinoderm can be spread as stable monolayers on 0.5 M NaCl solution at 298.2 K together with phospholipids. The π–A and ΔV–A isotherms of cerebrosides/DPPC mixtures show that the two components are miscible in the monolayer state over the whole range of DPPC mole fractions and of surface pressures investigated. From the A–$X_{phospholipid}$ and ΔV_m–$X_{phospholipid}$ plots, partial molecular surface area (PMA), and apparent partial molecular surface potential (APSP) were determined at the discrete surface pressure. The PMA changes with the mole fraction were extensively discussed for the miscible system. On the other hand, the APSP shows almost the original values over the whole mole fraction range for LMC-1/DPPC system, while the APSP for LMC-2/DPPC system changed depending upon the surface pressure. In contrast, binary systems of cerebrosides/DPPE suggest that the two components are completely immiscible in the monolayer state. The two-dimensional phase diagram and the Joos equation allowed calculation of the interaction parameter (ξ) and interaction energy ($-\Delta\varepsilon$) between cerebrosides and phospholipids for miscible binary systems. The two types of phase diagrams were obtained and were classified as follows: the positive azeotropic (cerebrosides/DPPC) and the completely phase separate types (cerebrosides/DPPE). The saccharide polar head group and the hydrophobic tail groups strongly influence the surface potential. The Demchak and Fort model was applied to analyze the surface potential of cerebrosides, from which the dipole moment of the polar head group was determined to be 0.63 D. Fluorescence microscopy for two-component cerebrosides/DPPC monolayers on 0.5 M NaCl solution showed that cerebrosides dissolve the LC domains formed upon compression of DPPC monolayer. In contrast, the FM images of the cerebrosides/DPPE systems showed immiscible pattern. These phenomena indicate that the miscibility of two-component system is influenced by an extent of hydrophilicity of polar head group.

Acknowledgements

This work was partially supported by Grant-in-Aid for Scientific Research from the Kieikai Foundation (Japan), which is greatly appreciated. We also thank Emeritus Prof. Y. Moroi (Kyushu University, Japan) for helpful and stimulating discussions about this manuscript.

References

[1] B. Alberts, Molecular Biology of the Cell, third ed., Garland Publishing, Inc., New York, 1994.
[2] B. Mggio, Prog. Biophys. Mol. Biol. 62 (1994) 55.
[3] R.A. Demel, Y. London, W.S.M. Geurts Van Kessel, F.G.A. Vossenberg, L.L.M. Van Deenen, Biochim. Biophys. Acta 311 (1973) 507.
[4] R. Koynava, M. Caffrey, Biochim. Biophys. Acta 1255 (1995) 213.
[5] S. Hakomori, Y. Igarashi, J. Biochem. 118 (1995) 1091.
[6] D. Pelled, H. Shogomori, A.H. Futerman, J. Inherit. Metab. Dis. 23 (2000) 175.
[7] K. Simons, E. Ikonen, Nature 387 (1997) 569.
[8] R.E. Brown, J. Cell Sci. 111 (1998) 1.
[9] D.S. Johnston, E. Coppard, D. Chapman, Biochim. Biophys. Acta 815 (1985) 325.
[10] D.S. Johnston, D. Chapman, Biochim. Biophys. Acta 937 (1988) 10.
[11] S. Ali, H.L. Brockman, R.E. Brown, Biochemistry 30 (1991) 11198.
[12] S. Ali, J.M. Smaby, H.L. Brockman, R.E. Brown, Biochemistry 33 (1994) 2900.
[13] S. Ali, J.M. Smaby, R.E. Brown, Thin Solid Films 244 (1994) 860.
[14] W. Stoffel, A. Bosio, Curr. Opin. Neurobiol. 7 (1997) 654.
[15] S. Figueroa-Perez, R.R. Schmidt, Carbohydrate Res. 328 (2000) 95.
[16] T. Tencomnao, R.K. Yu, D. Kapitonov, Biochim. Biophys. Acta 1517 (2001) 416.
[17] C.E.M. Hollak, E.P.M. Corssmit, J.M.F.G. Aerts, E. Endert, H.P. Sauerwein, J.A. Romijn, M.H.J. van Oers, Am. J. Med. 103 (1997) 185.
[18] T. Murakami, T. Shimizu, K. Taguchi, Tetrahedron 56 (2000) 533.
[19] S. Kawatake, K. Nakamura, M. Inagaki, R. Higuchi, Chem. Pharm. Bull. 50 (8) (2002) 1091.
[20] J.M. Lassaletta, R.R. Schmidt, Tetrahedron Lett. 36 (24) (1995) 4209.
[21] H. Löfgren, I. Pascher, Chem. Phys. Lipids 20 (1977) 273.
[22] J.M. Smaby, V.S. Kulkarni, M. Momsen, R.E. Brown, Biophys. J. 70 (1996) 868.
[23] C.R. Flach, R. Mendelsohn, M.E. Rerek, D.J. Moore, J. Phys. Chem. B 104 (2000) 2159.
[24] D.C. Carrer, B. Maggio, Biochim. Biophys. Acta 1514 (2001) 87.
[25] (a) M. Diociaiuti, I. Ruspantini, C. Giordani, F. Bordi, P. Chistolini, Biophys. J. 86 (2004) 321;

(b) J. Majewski, T.L. Kuhl, K. Kjaer, G.S. Smith, Biophys. J. 81 (2004) 2707;
(c) C.M. Rosetti, R.G. Oliveira, B. Maggio, Langmuir 19 (2003) 377.
[26] S. Nakamura, O. Shibata, K. Nakamura, M. Inagaki, R. Higuchi, Stud. Surf. Sci. Catal. 132 (2001) 447.
[27] R.J. Demchak, T. Fort Jr., J. Colloid Interf. Sci. 46 (1974) 191.
[28] R. Higuchi, M. Inagaki, K. Togawa, T. Miyamoto, T. Komori, Liebigs Ann. Chem. (1994) 653.
[29] (a) O. Shibata, Y. Moroi, M. Saito, R. Matuura, Langmuir 8 (1992) 1806;
(b) O. Shibata, M. Moroi, Y. Saito, R. Matuura, Thin Solid Films 242 (1994) 273;
(c) O. Shibata, H. Miyoshi, S. Nagadome, G. Sugihara, H. Igimi, J. Colloid Interf. Sci. 146 (1991) 595;
(d) H. Miyoshi, S. Nagadome, G. Sugihara, H. Kagimoto, Y. Ikawa, H. Igimi, O. Shibata, J. Colloid Interf. Sci. 149 (1992) 216;
(e) O. Shibata, Y. Moroi, M. Saito, R. Matuura, Thin Solid Films 123 (1998) 327;
(f) O. Shibata, M.P. Krafft, Langmuir 16 (2000) 10281.
[30] J.T. Davies, E.K. Rideal, Interfacial Phenomena, second ed., Academic Press, New York and London, 1963, p. 71.
[31] V. Vogel, D. Möbius, Thin Solid Films 159 (1988) 73.
[32] J.G. Petrov, E.E. Polymeropoulos, H. Möhwald, J. Phys. Chem. A 100 (1996) 9860.
[33] D.M. Taylor, O.N. Oliveira Jr., H. Morgan, J. Colloid Interf. Sci. 139 (1990) 508.
[34] M.K. Bernett, N.L. Jarvis, W.A. Zisman, J. Phys. Chem. 68 (1964) 3520.
[35] C.P. Smyth, Dielectric Behaviour and Structure, McGraw-Hill, New York, 1955.
[36] M.K. Bernett, W.A. Zisman, J. Phys. Chem. 67 (1963) 1534.
[37] (a) J. Marsden, J.H. Schulman, Trans. Faraday Soc. 34 (1938) 748;
(b) D.O. Shah, J.H. Schulman, J. Lipid Res. 8 (1967) 215.
[38] S. Yamamoto, O. Shibata, S. Lee, G. Sugihara, Prog. Anesth. Mech. (Special Issue) 3 (1995) 25.
[39] M. Kodama, O. Shibata, S. Nakamura, S. Lee, G. Sugihara, Colloid Surf. A 33 (2004) 211.
[40] C.A. Helm, H. Möhwald, K. Kjaer, J. Als-Niesen, Biophys. J. 52 (1987) 381.
[41] O. Albrecht, H. Gruler, E. Sackman, J. Phys. (France) 39 (1978) 301.
[42] V.M. Kagner, H. Möhwald, P. Dutta, Rev. Mod. Phys. 71 (1999) 779.
[43] Y.K. Levine, Prog. Surf. Sci. 3 (1973) 279.
[44] P. Joos, R.A. Demel, Biochim. Biophys. Acta 183 (1969) 447.
[45] C.W. McConlogue, T.K. Vanderlick, Langmuir 13 (1997) 7158.
[46] C.W. McConlogue, T.K. Vanderlick, Langmuir 14 (1998) 6556.
[47] C.W. McConlogue, D. Malamud, T.K. Vanderlick, Biochim. Biophys. Acta 1372 (1998) 124.
[48] J.M. Holopainen, J.Y.A. Lehtonen, P.K.J. Kinnunen, Chem. Phys. Lipids 88 (1997) 1.
[49] J.M. Holopainen, H.L. Brockman, R.E. Brown, P.K.J. Kinnunen, Biophys. J. 80 (2001) 765.